Arabian Journal for Science and Engineering (2023) 48:14183–14194
https://doi.org/10.1007/s13369-023-08121-z

RESEARCH ARTICLE-CIVIL ENGINEERING

Finite Element-Based p-y Curves in Sand

Murat Hamderi[1]

Received: 2 February 2023 / Accepted: 13 July 2023 / Published online: 3 August 2023

Abstract
P-y curves are used in the prediction of non-linear soil resistance resulting from the horizontal pile movement. Many of the p-y curves have been developed in the 1970s for the petroleum industry to predict the horizontal capacity of piles supporting oil platforms. These curves are based on the beam theory fed by strain-gauge data installed on several full-size pile tests. In this particular study, a p-y curve formula for sand was developed using 34 finite element combinations. The p-y curve formula includes the input of soil modulus, soil friction angle, soil unit weight and pile diameter. The results of the formula and the finite element program were validated against the test data available in the literature.

Keywords p-y curve · Pile · Lateral pile loading · Midas GTS NX

1 Introduction

The primary purpose of piles is to provide vertical support for heavy structures like tall buildings, towers, dams, bridge abutments, and power stations. These structures also occasionally experience horizontal loads such as wind and earthquake, which are transferred through piles to the ground. Additionally, the oil platforms in water also experience horizontal loads from waves and docked ships. The pile experiencing a horizontal load moves on the direction of the load at an amount of "y". In this case the soil around the pile develops resistance on the opposite side of the point of application. If the pile is treated as a beam, the lateral soil resistance can be defined in terms of line load per unit length, "p". The value of "p" is analogous to passive pressure, which is dependent on the amount of movement [1, 2]. Like in the passive pressure concept, the researchers focused on the ultimate lateral resistance of piles and offered several formulas for cohesionless soils. Brinch Hansen [3] offered a lateral earth pressure coefficient for piles, in which the ultimate pile resistance is calculated by multiplying the earth pressure coefficient with pile diameter, soil unit weight and the depth. In the same equation, Broms [4] employed three times the Rankine's passive pressure coefficient as the lateral earth pressure coefficient. Fleming et al. [5] offered the same value as the square of the Rankine's passive pressure coefficient. Reese et al. [6] calculated the same value in terms of soil friction angle, Rankine's active pressure coefficient and the coefficient of earth pressure at rest. In addition, Reese et al. [6] offered nonlinear p-y curves for sand. To determine the pile movement or deflection "y," Reese et al. [6] utilized large-size piles that were equipped with strain gauges to measure the moment distribution along the pile. By applying specific boundary conditions and performing double numerical integration of the moment measurements, they were able to calculate the pile's movement or deflection "y." By performing a double derivative of the moment, Reese et al. [6] obtained the lateral soil resistance "p" with a certain level of accuracy. Another study by Zang [7] includes the elastoplastic semi-analytical solutions of lateral pile response under vertical and lateral loads.

Reese et al.'s method of deriving p-y curves for sand, which is based on full-size tests and employs a nonlinear formulation, continues to be widely used in practical applications. This approach, due to its reliance on real-scale experiments and its ability to capture nonlinearity, remains a prevalent and valuable method in the field. Besides a few numbers of full-size tests, there are also a couple of laboratory tests focusing on horizontal pile loading [8–12]. Centrifugal laboratory tests have also been conducted to study p-y curves [13, 14]. Bouzid [15] employed the finite element method with Fourier series to derive p-y curves for pile segments. A

✉ Murat Hamderi
hamderi@tau.edu.tr

[1] Civil Engineering Department, Faculty of Engineering, Turkish-German University, Istanbul, Turkey

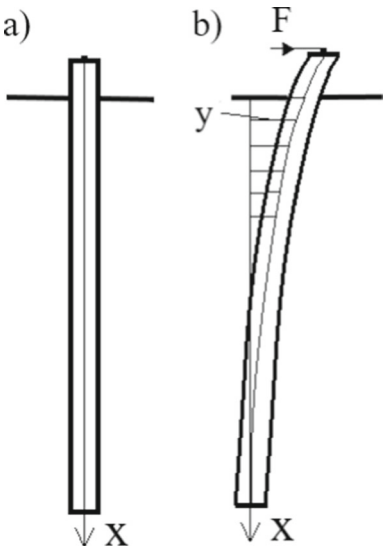

Fig. 1 A pile, **a** at rest with no horizontal deformation, **b** under the effect of a horizontal load creating a horizontal deformation "y" which is a function of depth "x"

more recent approach involved the use of tuned mass dampers to determine spring coefficients using p-y curves [16].

While the beam theory has proven valuable in the development of p-y curves for practical applications, it is important to note that the problem of determining lateral pressure in relation to pile deflection is inherently a three-dimensional (3D) problem. The beam theory simplifies the problem by assuming one-dimensional behavior along the length of the pile, neglecting the complexities introduced by lateral variations. However, in reality, the interaction between the pile and soil is a complex 3D phenomenon that requires more sophisticated approaches, such as advanced computational models, to accurately capture the true behavior of the system. Nowadays, using advanced computational power, it is possible to create 3D models of pile-soil interaction. In the study, a nonlinear p-y curve formula for sand was developed using thirty-four 3D finite element (FE) model configurations. The p-y curve formula includes the input of soil modulus, soil friction angle, soil unit weight and pile diameter. The FE model was validated against the laboratory test performed by Meyerhof and Sastry [9]. The formula's predictions for the ultimate lateral soil resistance were also compared with values available in existing literature, ensuring the accuracy and reliability of the developed formula.

2 Statement of the Problem

A pile standing at rest such as demonstrated in Fig. 1a. has a circular uniform lateral earth pressure acting on its body (Fig. 2a). When a horizontal force applied on the top, it

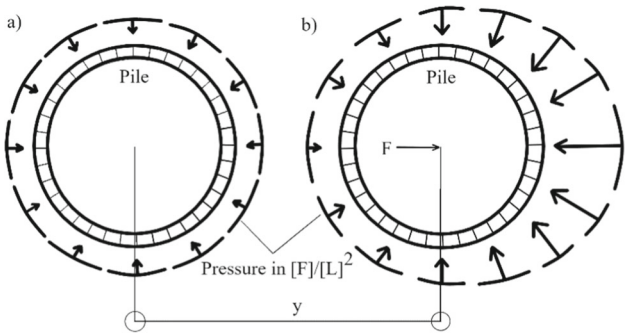

Fig. 2 Pressure distribution around **a** a pile at rest, **b** a pile under the effect of a horizontal load [17]

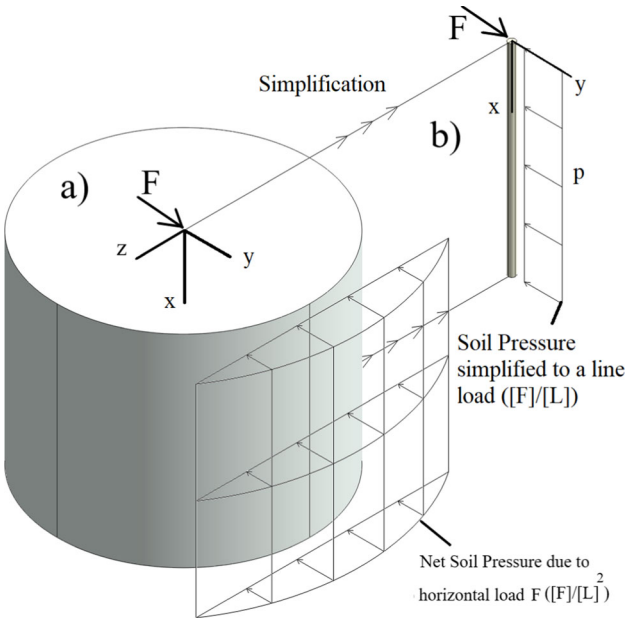

Fig. 3 **a** Net soil pressure due to horizontal load F in 3D environment, **b** Net soil pressure simplified to a line load to be used with beam theory

deflects at an amount of "y" (Fig. 1b). As the depth "x" increases, the amount of deflection decreases. When a horizontal load is applied, the circular and uniform shape of the lateral load is altered, causing it to bulge towards the opposite side of the load application point. This phenomenon can be observed in Fig. 2b [2]. In this scenario, the net horizontal lateral pressure exhibits a profile similar to the one depicted in Fig. 3a. It is important to note that the pile is treated as a three-dimensional structure, and as a result, the conventional beam theory principles used to calculate moment along the pile length do not apply. By integrating the pressure distribution shown in Fig. 3a in the "z" direction, a line-type soil resistance "p" can be obtained, represented in units of [F]/[L], as illustrated in Fig. 3b. The soil resistance "p" varies along the depth "x" of the pile. Consequently, p-y curves need to be generated at specific intervals corresponding to different depths

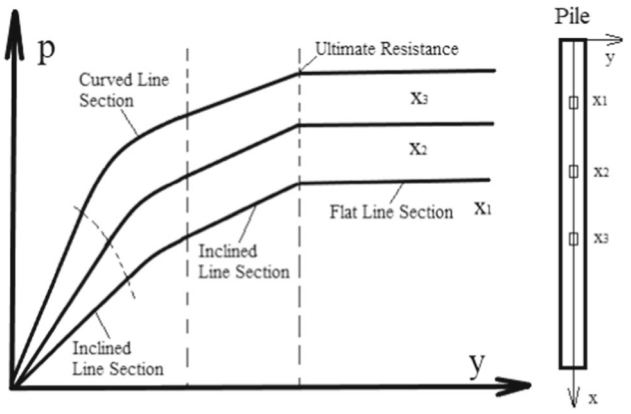

Fig. 4 Characteristic shape of p-y curves offered by Reese et al., [6]

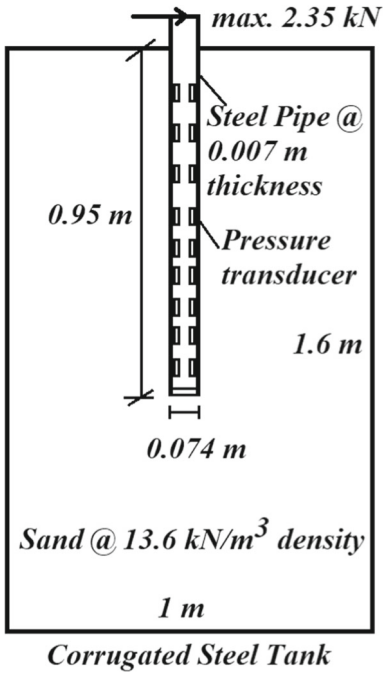

Fig. 5 The general view of the test facility [9]

to accurately capture this variation in soil resistance with depth. The characteristic shape of p-y curves by Reese et al. [6], which are widely used in current practice, are demonstrated in Fig. 4. The curves are given for various depths. As the depth increases the ultimate resistance increases. The curve has an inclined line section at the beginning, then a curved section, followed by an inclined line section and finally a flat section. The start of the curved section is variable with depth; however, the start and end points of the second inclined linear section are constant for all depths (Fig. 4). The p-y curve is obtained using the input parameters such as soil friction angle, Rankine's active pressure coefficient and the coefficient of earth pressure at rest. The initial inclined section of the p-y curve is a function of the soil modulus. Soil modulus is defined in terms of bedding coefficient in $[F]/[L]^3$. The bedding coefficients for loose, medium and dense sands are provided in the reference. The procedure described here has been offered 50 years ago and it is still widely practiced by engineers. However, with the increasing computing power, this procedure can be further advanced. For this purpose, in this study, a new p-y curve formula has been developed based on 34 FE model configurations in Midas GTS NX program. The formula developed using the power of 3D finite element (FE) modeling is well-suited to meet the requirements of modern engineering practice. Its derivation through rigorous modeling techniques ensures its applicability and accuracy in practical scenarios. The validation of the FE model, as well as the subsequent development and application of the formula, are presented and discussed in the following sections of the study.

3 Validation of the FE Model

The FE program MIDAS GTS NX (ver. 2019-1.1), which was used in the derivation of the p-y formula, will be validated against the laboratory horizontal loading test by Meyerhof and Sastry [9]. The main goal is to create a reasonably identical model of the reference laboratory test and compare the results. Meyerhof and Sastry applied vertical eccentric and centric inclined loads to a steel pile in 0.007 m wall thickness, 1.1 m in length and 0.074 m in diameter (Fig. 5). The 0.95 m long portion of the pile was embedded in sand with an effective grain size D_{10} of 0.38 mm, uniformity coefficient of C_u of 2.8, triaxial test internal friction angle of 30°. The relative density of sand was around 20%, which is classified as loose sand. The sand was contained in a corrugated steel drum in 1 m diameter and 1.6 m height. The sand was funneled into the drum to obtain a density of 13.6 kN/m^3. The pile was jacked into the soil at a rate of 13 mm/min. Of the various loading conditions, the horizontal centric loading condition was incorporated in the validation. The horizontal failure load was 2.35 kN. During the loading, the soil resistance was measured with pressure transducers on both sides at various depths as depicted in Fig. 5.

After the completion of pile loading tests, a cone penetrometer test (CPT) was performed in the vicinity of the test pile. The CPT results are demonstrated in Fig. 6. In the scope of this study, two linear curves were fitted to the Meyerhof and Sastry's CPT data to obtain cone resistance q_c as depicted in Fig. 6.

The FE model of Meyerhof and Sastry's test was created according to the provided data in the reference paper. The FE model dimensions were set to match the parameters used in the original laboratory test. The steel drum around the sand was not modelled directly, instead of this, vertical and

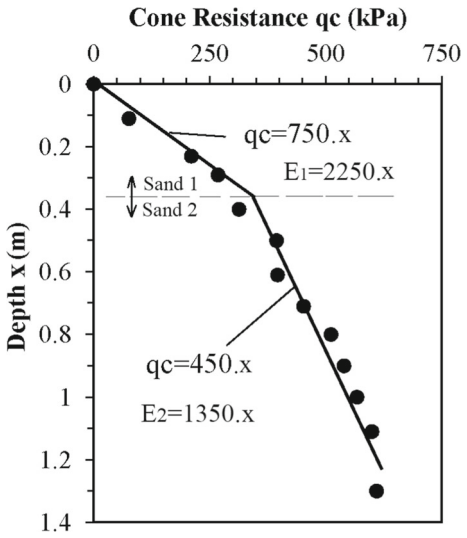

Fig. 6 The cone resistance plot in the Meyerhof and Sastry's test and fitted two curves

horizontal boundaries were employed on the sides and the bottom (Fig. 7a.). The steel pile was modelled with linear elastic material with an elastic modulus of 210 000 MPa. The Mohr–Coulomb soil model was employed for sand. The soil modulus of the sand was calculated according to the CPT data. As demonstrated in Fig. 6., there are two zones for sand, at both zones the cone pressure value increases linearly but at different rates. The cone pressure value in the first and the second zone can be approximated with the following formulas, respectively: $qc_1 = 750x$, and $qc_2 = 450x$. As reported by Bowles, the soil modulus value of sand corresponds to three times of its cone resistance value [18]. Therefore, the soil modulus of the first and the second zones are calculated as $E_1 = 2250x$, and $E_2 = 1350x$. Thanks to the variable soil modulus option of the FE program, these two equations could directly be incorporated into the soil modulus. The soil media was meshed with tetrahedral and hexahedral elements with mid-side nodes.

In the actual test by Meyerhof and Sastry, the sand was deposited by funnel into the steel drum. In the FE program, this corresponds to the initial stage, where only sand layers were activated to generate initial stresses. During this stage, the coefficient of lateral earth pressure k_o was set to 0.5. During the actual test, the hollow pipe section was jacked into the ground. Jacking is known to generate compaction in the ground. In the FE model, this was not possible, therefore, in the second stage the material property of the sand volume corresponding to the location of the steel pipe was set to steel (Fig. 7b). It is believed that the compaction effect of jacking has been reflected in the final soil modulus value, because the CPT test data was obtained after the jacking of the pile. In the last stage, the 2.35 kN point load equivalent surface load of 1571.5 kPa was introduced into the system in ten steps. In the FE model, the steel pile was surrounded by an interface. The interface was useful in reading the lateral pressure between soil and steel pile. The pressure readings were taken at the locations where there are actual pressure transducers in the reference test. Two example locations are demonstrated in Fig. 7c. The lateral earth pressures obtained from FE model and the test are plotted in Fig. 8. The general

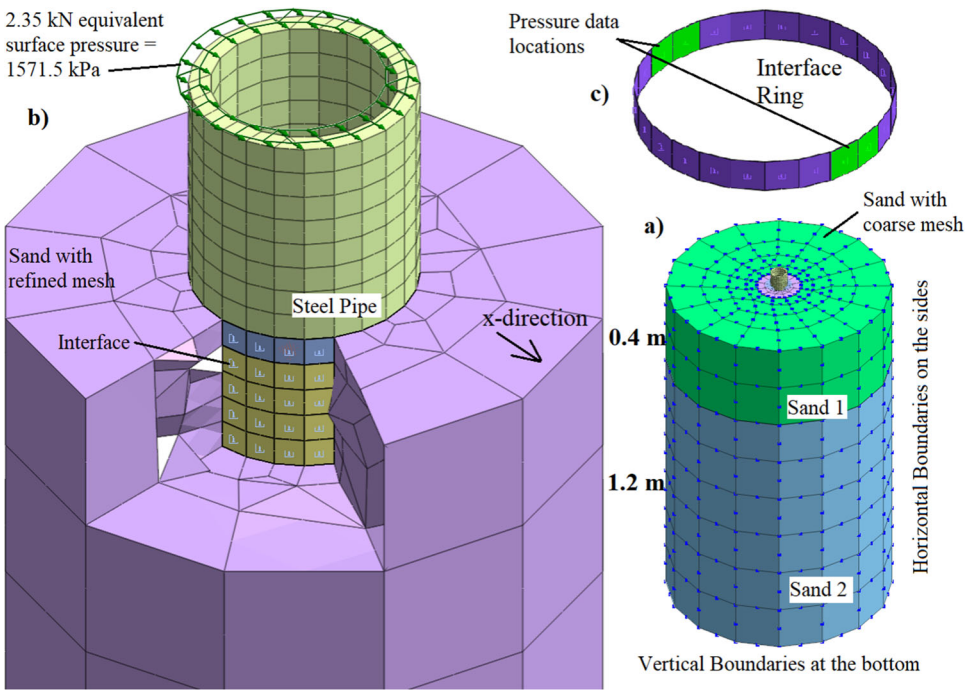

Fig. 7 The details of the FE model of the test by Meyerhof and Sastry [9] **a** the general view of the mesh, **b** the view of the inner purple section including the pile, **c** an interface ring surrounding the pile

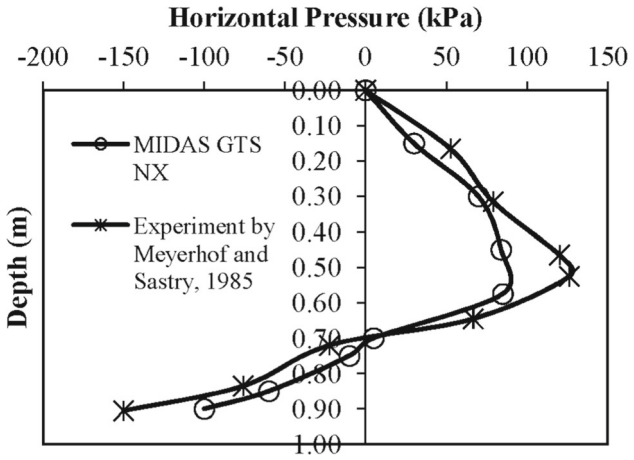

Fig. 8 The lateral pressure plots of the FE validation model and the test by Meyerhof and Sastry [9]

shape of both curves is very similar, especially the maximum point and the point where the line intersects the y axis. Although the location of important points coincides, there are deviations at the maximum values on the right and the left side. It would be very surprising if these points coincide exactly using the soil modulus correlated from CPT data. Overall, the FE program and the reference test are in good agreement in terms of geotechnical point of view. This indicates that the 3D model, when coupled with Mohr–Coulomb soil properties, can accurately replicate the behavior of a pile under horizontal loading conditions.

4 The Setup of FE Model for Formula Derivation

The p-y formula was derived by analyzing data from 34 different combinations of finite element (FE) models. These combinations include various pile diameters, soil moduli E, soil internal friction angles ϕ, soil unit weights γ. If the soil is saturated with water the effective soil unit weight should be used. The soil around the pile has been divided into 4 zones, which were 3 m, 3 m, 6 m and 8 m in height (Fig. 9). By employing this approach, specific soil moduli and internal friction angles can be assigned to the different layers within the FE models. In the 34 FE model combinations, while specific values for soil modulus and internal friction angle were assigned to each soil layer, the soil unit weight (γ) remained consistent across all the layers. The input parameter details for these 34 FE model combinations, including soil modulus, internal friction angle, and other relevant information, can be found in Table 1.

The general mesh view of the FE model for the formula derivation is demonstrated in Fig. 10a. The soil layers mentioned earlier are shown in different colors. A more detailed

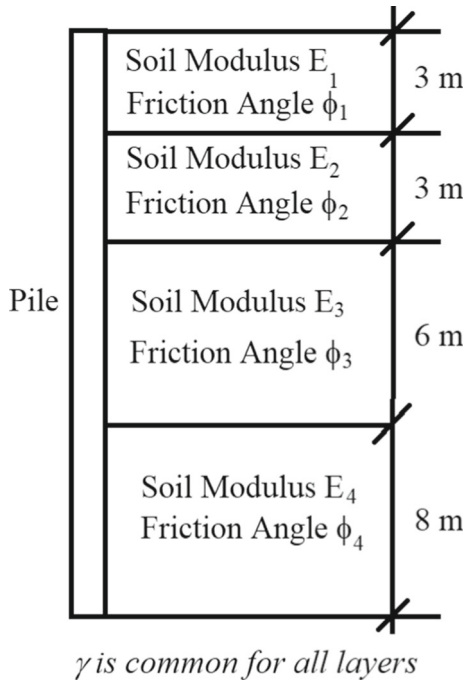

Fig. 9 Demonstration of soil layers around the 20 m-long pile

view of the mesh is demonstrated in Fig. 10b. Based on the provided figure, it is evident that the pile is centrally positioned within the soil media. The length of the pile was constant and 20 m. The diameter "D" of the pile was variable, briefly, 0.25 m, 0.5 m, 1 m and 1.5 m at various FE model configurations. The side length of the soil media was set to 4 times of the diameter. The height of the soil media was 25 m. A pattern-type mesh was employed in the analysis, consisting of large hexahedral elements surrounding the sides of the model. In the vicinity of the pile, a finer mesh was utilized, incorporating either hexahedral or tetrahedral elements. The inner side of the pile was filled with cotton-like elastic element with a unit weight set equal to that of the soil in the vicinity. This provided proper generation of initial stresses. The utilization of a cotton-like elastic element, characterized by a very low modulus of elasticity, within the pile is justified and will be further explained in the following paragraphs.

In the validation model of the pile with an embedded depth of 0.95 m, the horizontal pressure distributed along the pile's entire depth. However, if that pile was wider and longer such as 0.5 m in diameter and 10 m in length, unlike the small test pile, the pressure increase due to horizontal load would be much more concentrated within the first 2–3 m length of the 10 m-long pile. Such a concentration scheme is also valid for the horizontal deflection "y". Briefly, the deflection would be much higher at the top sections, whereas it would be much smaller at lower sections. If the p-y curves at various depths would like to be obtained from a horizontally loaded pile, it would be possible to obtain p-y curves for the first

Table 1 The input parameter details of 34 FE model combinations

No	Soil Modulus (1000 × kPa)	int. friction (°)	Dia.(m)	Unit W. (kN/m^3)
1–4	(E_1, E_2, E_3, E_4) = (10,10,10,10), (25, 25, 25,25), (50, 50, 50,50), (100, 100, 100,100)	(ϕ_1, ϕ_2, ϕ_3, ϕ_4) = (34°,34°,34°,34°)	D = 1.5	γ = 16
5–8	(E_1, E_2, E_3, E_4) = (10,10,10,10), (25, 25, 25,25), (50, 50, 50,50), (100, 100, 100,100)	(ϕ_1, ϕ_2, ϕ_3, ϕ_4) = (34°,34°,34°,34°)	D = 0.25	γ = 16
9–13	(E_1, E_2, E_3, E_4) = (25,50,50,50), (25, 25, 50, 50), (50, 25, 25, 25), (10, 25, 50, 100), (50, 60, 75, 100)	(ϕ_1, ϕ_2, ϕ_3, ϕ_4) = (34°,34°,34°,34°)	D = 0.25	γ = 16
14–17	(E_1, E_2, E_3, E_4) = (25,25,25,25)	(ϕ_1) = 30, 26, 38, 42, (ϕ_2, ϕ_3, ϕ_4) = (34,34,34)	D = 0.25	γ= 16
18–24	(E_1, E_2, E_3, E_4) = (25,25,25,25)	(ϕ_1, ϕ_2, ϕ_3, ϕ_4) = (32°,32°,32°,32°), (36°,36°,36°,36°), (38°,38°,38°,38°), (40°,40°,40°,40°), (42°,42°,42°,42°), (44°,44°,44°,44°), (32°,35°,38°,41°)	D = 0.25	γ= 16
25–28	(E_1, E_2, E_3, E_4) = (25,25,25,25)	(ϕ_1, ϕ_2, ϕ_3, ϕ_4) = (34°,34°,34°,34°)	D = 0.25	γ= 14, 18, 20, 22
29–30	(E_1, E_2, E_3, E_4) = (25,25,25,25)	(ϕ1, ϕ2, ϕ3, ϕ_4) = (34°,34°,34°,34°)	D = 0.5, 1	γ = 16
31	(E_1, E_2, E_3, E_4) = (50,50,50,50)	(ϕ_1, ϕ_2, ϕ_3, ϕ_4) = (34°,34°,34°,34°)	D = 0.25	γ' = 6
32–34	(E_1, E_2, E_3, E_4) = (25,25,25,25)	(ϕ_1, ϕ_2, ϕ_3, ϕ_4) = (34°,34°,34°,34°)	D = 0.5, 1, 1.5	γ' = 6

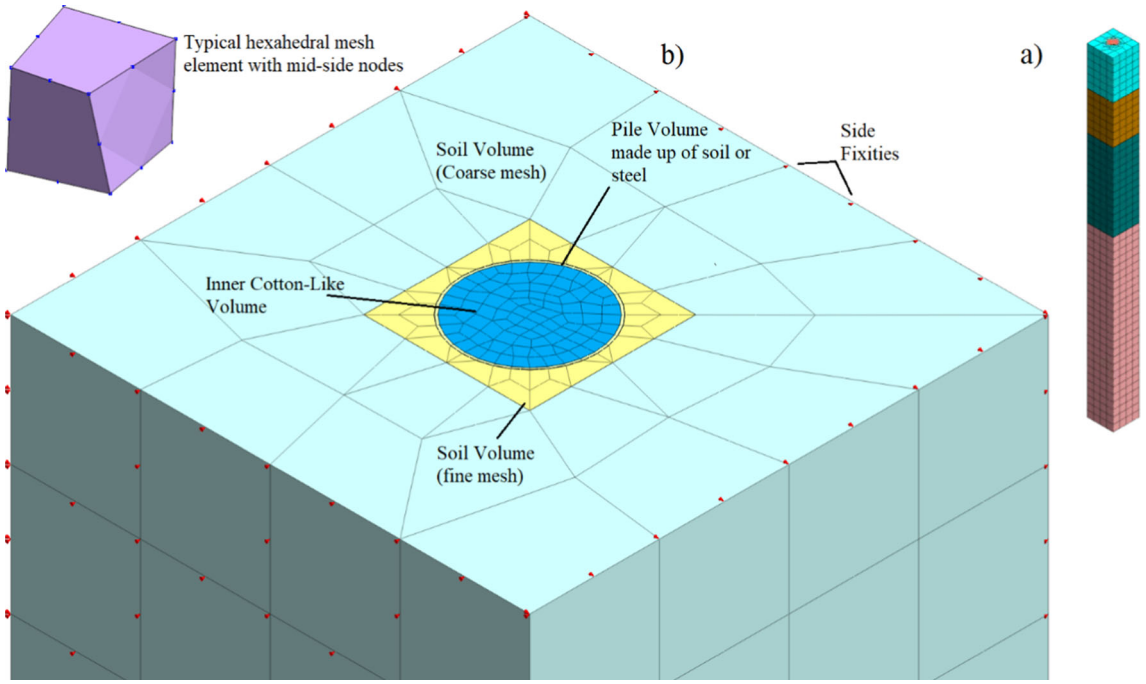

Fig. 10 **a** General, **b** detailed mesh of view the 34 FE model combinations

2–3 m, however, at lower depths, this is not possible, since the deflection y is too small. In other words, p-y curve at lower depths such as demonstrated in Fig. 4 cannot be completed due to insufficient large y values. To overcome this issue, instead of loading a monolithic pile horizontally from the top, a prescribed displacement was applied to a pile ring section in 0.05 m height at every 0.5 or 1 m. Such a pile ring is demonstrated in Fig. 11. The prescribed displacement had a maximum value of 0.03 m and was applied in 10 steps. The locations of these rings on the pile volume are demonstrated in Fig. 12.

Similar to the validation model, a staged construction procedure was implemented in the finite element (FE) models used for deriving the p-y formula. In the first stage, initial

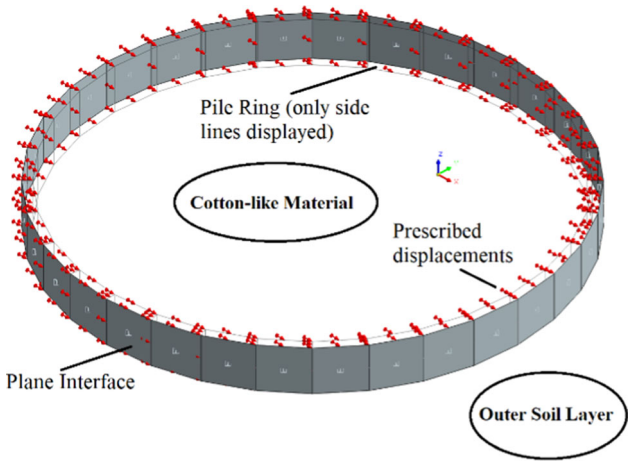

Fig. 11 A pile ring along with an interface surrounding it, subjected to horizontal prescribed displacement

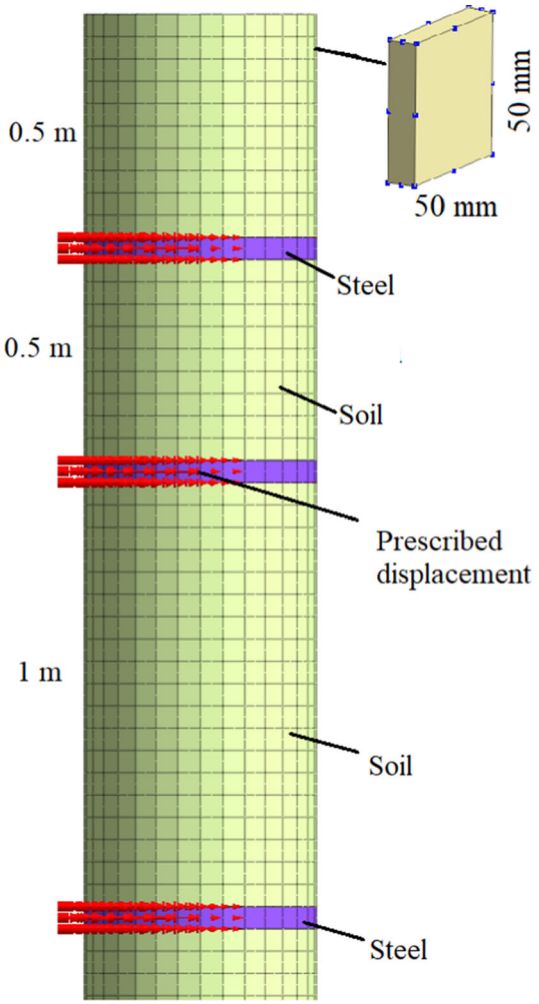

Fig. 12 The longitudinal view of the pile body demonstrating the locations of steel rings

stresses were developed by assigning Mohr–Coulomb soil properties to the entire volume except the inner cotton-like volume demonstrated in Fig. 10b. In the modeling process, the generated displacements were initially set to zero, indicating the initial state of the system. In the second stage, the properties of the volumes corresponding to the ring locations were changed to simulate the presence of steel material (as shown in Fig. 12). Similarly, in this stage, the generated displacements were again set to zero to maintain the initial equilibrium.

In the third stage, a horizontal displacement was applied to the steel rings in the x direction. This displacement was incrementally increased in ten steps, with each step corresponding to a displacement of approximately 0.03 m. In other words, "y" values of p-y curve become simply the multiples of 0.003 m. s the net pressure resistance develops around the steel ring, it can be divided by the diameter D of the ring to obtain the corresponding "p" value of the p-y curve. This "p" value represents the lateral soil resistance exerted on the pile per unit length. Furthermore, the presence of the steel ring also results in the dragging of the cotton-like material from both the top and bottom sides. Since the modulus of elasticity of this material was set to a very low value, the resistance contribution from this material is negligible. The net soil resistance, that the pile ring experiences, is calculated by summation of pressures in the x direction acting on the plane interface elements around steel ring. This is analogous to the net-pressure demonstrated in Fig. 3.

5 Formula Description

The formula was derived from the output data of the 34 FE model configurations by implementing multivariable regression analyses. The list of input parameters used in various combinations are given in Table 1. In each model combinations, a group of data (240 count) composed of x, y and p values were generated. The total number of data couples for 34 FE model configurations were 8160. The Solver function in MS Excel® was employed for regression analyses. The details of the regression analyses are presented in Appendix S1. The lateral soil resistance p (in [kN/m]) can be estimated with the following equation:

$$p = \frac{x^a * y^b}{\left(c + d * x^e * y^f\right)} * D^{(g+1)} * \left(\frac{E_n}{10^5}\right)^h * \left(\frac{\phi_n}{34}\right)^i * \left(\frac{\gamma}{16}\right)^j \quad (1)$$

where a, b, c, d, e, f, g, h, i and j are the fitting coefficients (Table 2), x (in [m]) is the depth, y (in [m]) is the deflection of pile at a certain depth x, E_n (in [kN/m^2]) is soil modulus at layer n, n is 1, 2, 3 and 4, ϕ_n is the internal friction angle of soil at layer n and γ is the unit weight of soil (([kN/m^3]),

Table 2 The fitting coefficients of the p-y equation

Range of x	a	b	c	d	e
$0.0001 \leq x < 3$	0.174376	0.846639	0.000038	0.009134	− 2.376373
$3 \leq x < 6$	0.205362	0.807185	0.000036	0.005577	− 5.268525
$6 \leq x < 9$	0.202343	0.807301	0.000034	0.005577	− 5.268525
$9 \leq x \leq 20$	0.253022	0.810901	0.000038	0.005577	− 5.268525
Range of x	f	g	h	i	j
$0.0001 \leq x < 3$	1.382370	− 0.424825	0.464454	1.088613	0.514760
$3 \leq x < 6$	5.903368	− 0.279820	0.600173	1.132096	0.256712
$6 \leq x < 9$	5.903368	− 0.211116	0.580252	0.977143	0.140122
$9 \leq x \leq 20$	5.903368	− 0.193878	0.579500	0.825870	0.146984

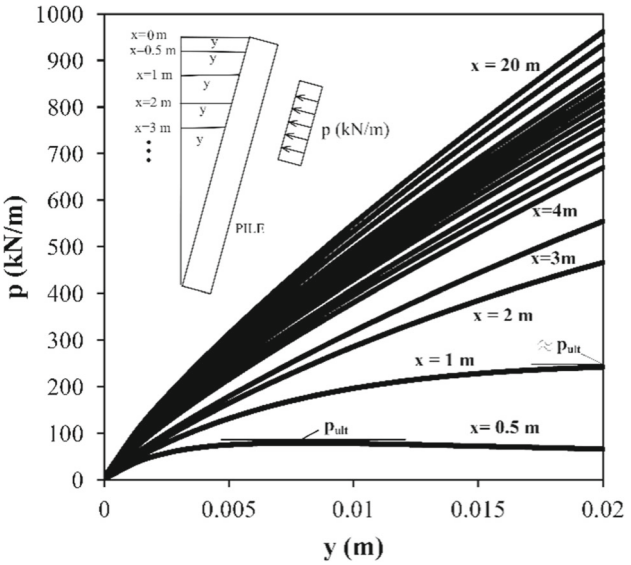

Fig. 13 p-y curves at various x depths including the parameters, E_n = 50,000 kPa, $\phi_n = 35°$, = , γ18 kN/m.^{3}, D = 0.25

see Fig. 9.). The effective unit weight should be considered if the soil is saturated with water.

6 Results and discussions

6.1 Influences of Input Parameters on p Value

In this section, some p-y curves will be plotted using the formula given in Eq. 1. Figure 13 demonstrates the p-y curves at different x depths for the constant values of $E_n = 50{,}000$ kPa, $\phi_n = 35°$, $\gamma = 18$ kN/m^3, D = 0.25 m. The curve at x = 0.50 m has a nonlinear shape, which flattens at around 0.005 m of displacement. The ultimate p value at x = 0.50 m is 70 kPa. The curve at x = 1 m has also a nonlinear shape, but it flattens at a much greater displacement, which is about 0.02 m. The ultimate p value is greater than 200 kPa. At greater depths the nonlinearity diminishes, the reached p values are greater, but the flattening of the curve occurs at a greater displacement.

This can be explained by examining the total displacement shadings presented in Fig. 14. Due to the prescribed displacements induced on the pile rings, displacement wedges move toward to the top of soil strata, where the confining pressure is low. This is analogous to the bearing capacity failure of a footing. At early stages the wedge formation is only apparent for the depths of 0.5 m and 1 m (Fig. 14a). In the final stage of the displacement loading, a wedge starts to appear for the depths of 2 m and 3 m. The depths, where the wedges are apparent, the p-y curves have a flattening trend (Fig. 13). For example, the curve for the depth of 2 m has not fully flatten yet, because the wedge has not been fully developed (Fig. 14b).

Unlike the curves offered in this study, the peak strength values of the p-y curves offered by Reese et al. [17] include a constant strain level (or displacement level) for peak strength (ultimate resistance, see Fig. 4).

The change of p value with the increasing soil modulus is demonstrated in Fig. 15. The soil modulus value ranged between 20 and 80 MPa. Other parameters were kept constant (x = 1 m, $\phi_n = 35°$, $\gamma = 18$ kN/m^3, D = 0.50 m). According to Fig. 15, the ultimate p value as well as the initial slope have a declining increase with increasing soil modulus value.

The change of p value with the increasing soil friction angle is demonstrated in Fig. 16. The soil friction angle ranged between 30° and 42°. Other parameters were kept constant (x = 1 m, $E_2 = E_3 = E_4 = 50{,}000$ kPa, $\gamma = 18$ kN/m^3, D = 0.50 m). According to Fig. 16, the ultimate p value as well as the initial slope had a constant increase with increasing soil friction value.

Similarly, the unit weight of soil (γ) was changed within the range of 14–20 kN/m^3. There is a minor increase in p value with increasing γ value (Fig. 17).

Finally, the change of p value with increasing pile diameter is demonstrated in Fig. 18. As expected, p value increases

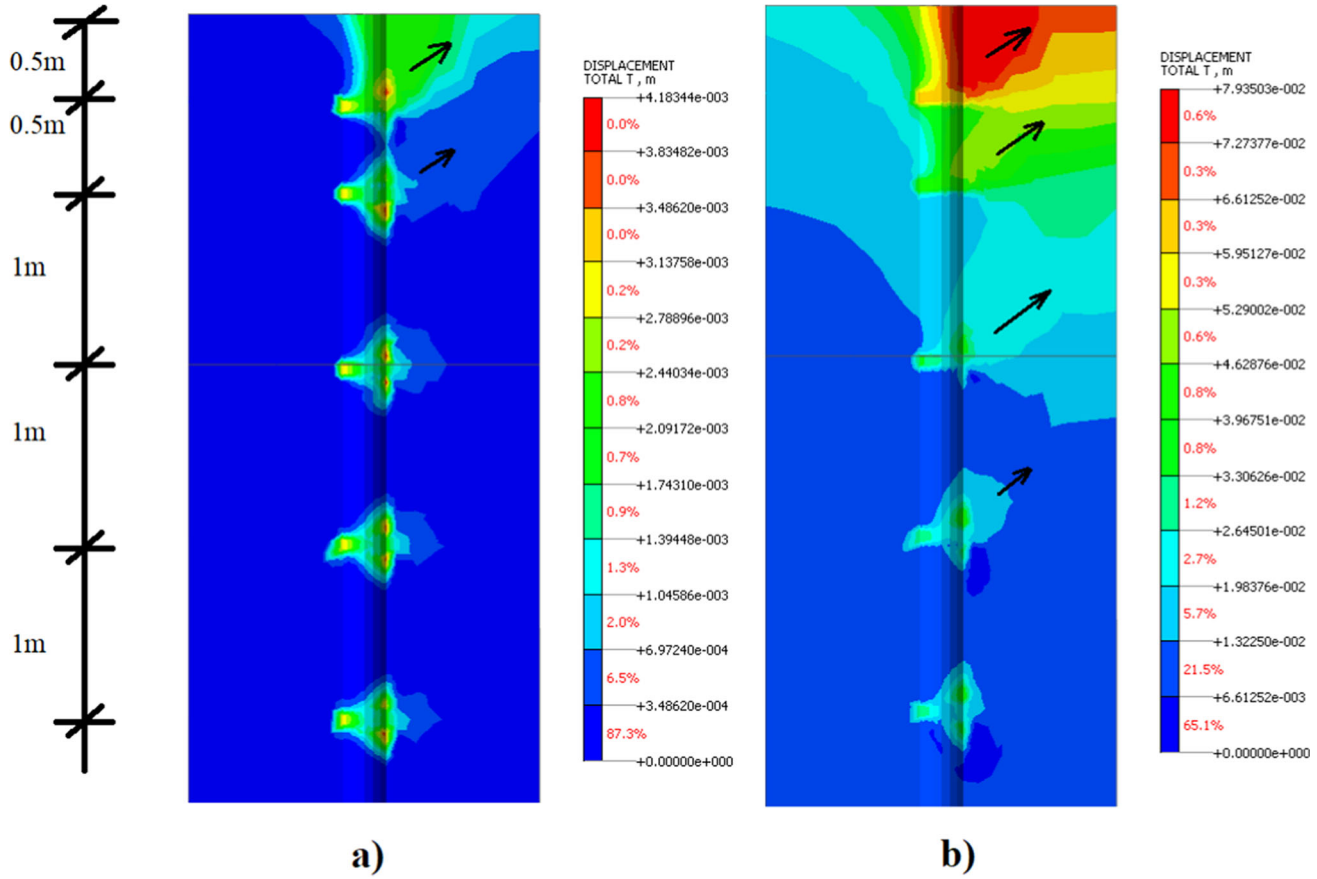

Fig. 14 The total displacements of pile rings: **a** at early displacement stages, **b** at further displacement stages

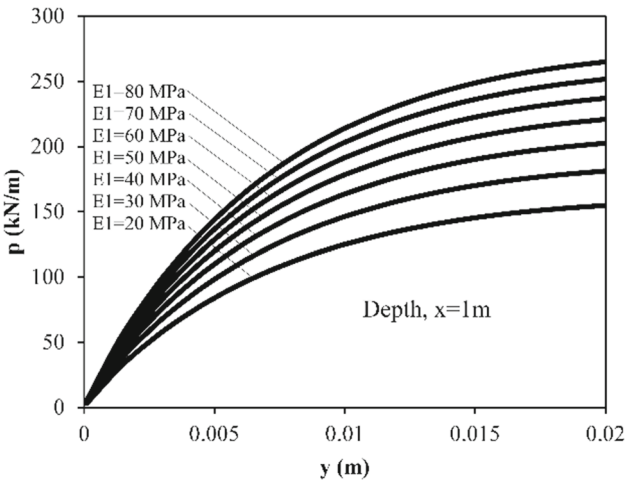

Fig. 15 p-y curves at various E_1 values including the parameters, x = 1 m, $\phi_n = 35°$, $\gamma = 18$ kN/m^3, D = 0.50 m

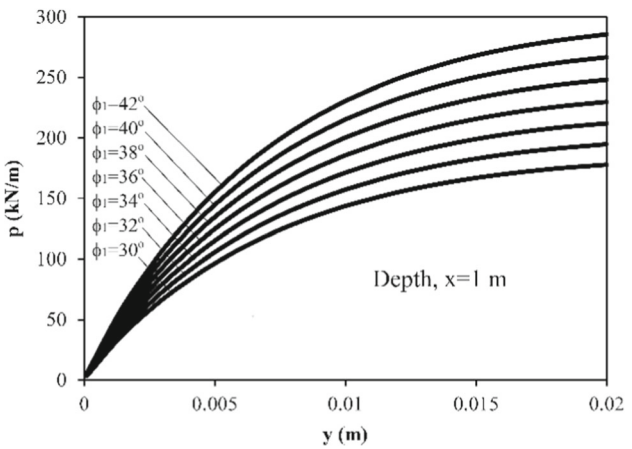

Fig. 16 p-y curves at various ϕ_1 values including the parameters, x = 1 m, $E_2 = E_3 = E_4 = 50{,}000$ kPa, $\gamma = 18$ kN/m^3, D = 0.50 m

with increasing pile diameter. However, the average lateral pressure on the pile, p/D (kN/m^2) has an opposite trend. As the diameter increases, the average lateral pressure decreases (Fig. 19).

6.2 Ultimate lateral resistance p_{ult}

In the literature, the ultimate lateral resistance p_{ult} has been estimated by several researchers. Brinch Hansen offered the following expression for p_{ult} [3]:

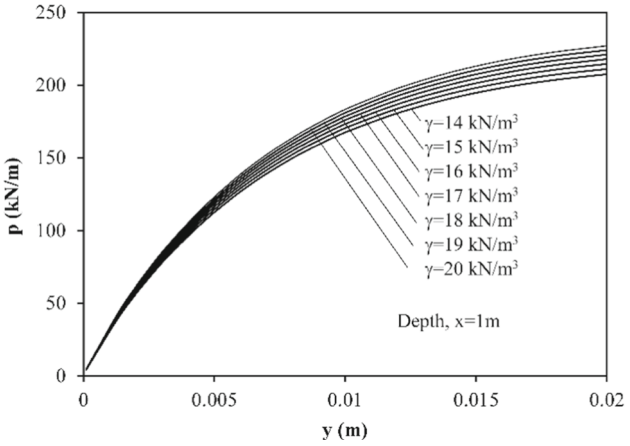

Fig. 17 p-y curves at various γ values including the parameters, x = 1 m, $\phi_n = 35°$, $E_n = 50{,}000$ kPa, D = 0.50 m

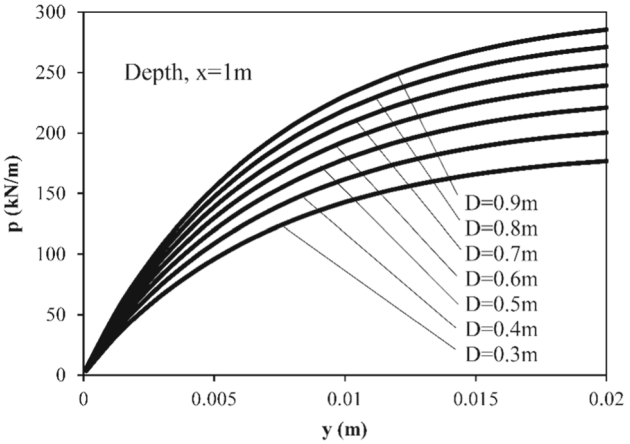

Fig. 18 p-y curves at various D values including the parameters, x = 1 m, $\phi_n = 35°$, $E_n = 50{,}000$ kPa, $\gamma = 18$ kN/m.^{3}

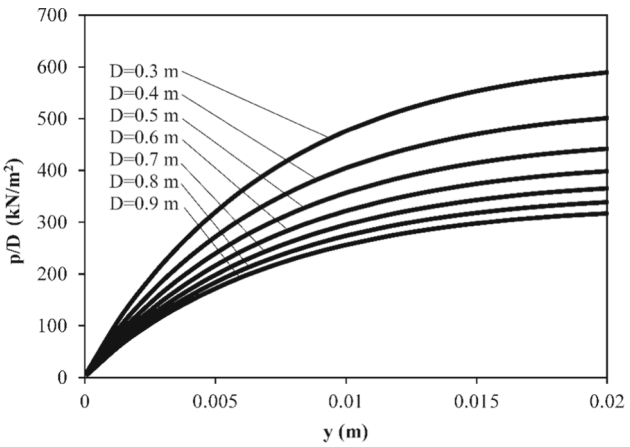

Fig. 19 P/D-y curves at various D values including the parameters, x = 1 m, $\phi_n = 35°$, $E_n = 50{,}000$ kPa, $\gamma = 18$ kN/m.^{3}

$$p_{ult-Hansen} = K_q.\Upsilon.x.D \tag{2}$$

where K_q = Brinch Hansen's earth pressure coefficient as a function of internal friction angle, γ = unit weight of soil, x = depth and D = pile diameter.

Broms used three times of Rankine's passive pressure coefficient value ($K_p = \tan^2(45° + \phi/2)$) and suggested the following formula [4]:

$$p_{ult-Broms} = 3K_p.\Upsilon.x.D \tag{3}$$

Fleming et al. offered the same value replacing the $3K_p$ term with $(K_p)^2$ [5]:

$$p_{ult-Fleming} = {K_p}^2.\Upsilon.x.D \tag{4}$$

Reese et al. calculated the same value in terms of soil friction angle, Rankine's active pressure coefficient and the coefficient of earth pressure at rest [6]. Reese et al. gave the ultimate resistance near and below the ground surface in Eq. 5 and Eq. 6, respectively as [6]:

$$\begin{aligned} p_{ult-Reese\ near} = \gamma.x.\Bigg[& \frac{K_o.x.\tan(\phi).\sin(45+\frac{\phi}{2})}{\tan\left(45-\frac{\phi}{2}\right).\cos(\frac{\phi}{2})} \\ & + \frac{\tan\left(45+\frac{\phi}{2}\right)}{\tan\left(45-\frac{\phi}{2}\right)} \\ & (D + x.\tan\left(45+\frac{\phi}{2}\right).\tan\left(\frac{\phi}{2}\right)) \\ & + K_o.x.\tan(45+\frac{\phi}{2}).(tan(\phi).sin(45 \\ & + \frac{\phi}{2}) - tan(\frac{\phi}{2})) - K_a.D\Bigg] \end{aligned} \tag{5}$$

$$\begin{aligned} p_{ult-Reese\ below} = D.\gamma.x.\Big[& K_a.\left(tan^8\left(45+\frac{\phi}{2}\right)-1\right) \\ & + K_o.\left(tan(\phi).tan^4\left(45+\frac{\phi}{2}\right)\right)\Big] \end{aligned} \tag{6}$$

where K_o = the lateral earth pressure coefficient at rest = 0.4 and K_a = Rankine's active lateral earth pressure coefficient = $\tan^2(45° - \phi/2)$.

The plots of the ultimate lateral resistance values for a pile with D = 0.5 m, $\phi = 35°$, $\gamma = 18$ kN/m^3 according to the various researchers are demonstrated in Fig. 20. It should be here noted that p_{ult} value is analogous to passive pressure, which only occurs at large displacements [2]. According to Fig. 20, the p_{ult} values offered by Broms and Fleming et al. are quite close whereas Brinch Hansen's and

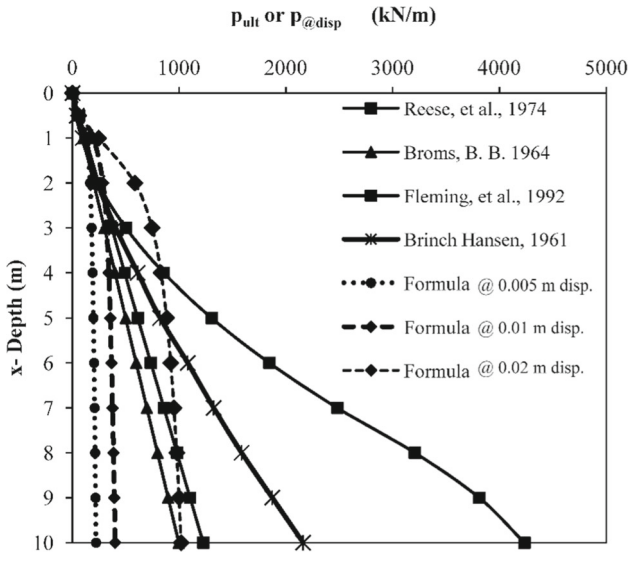

Fig. 20 Ultimate lateral resistance p_{ult} and soil resistance at a given displacement $p_{@disp}$

Reese, et. al.'s estimations yield greater p_{ult} values. Generally, the p_{ult} value increases with depth. Understanding the p_{ult} value at a certain depth might be challenging. Let's say 2% axial strain is allowed at a certain granular soil. A pile in 10 m in length and 0.5 m in diameter is pushed from the top until 2% strain occurs within the first 2 m depth. According to various researchers, the p_{ult} value at 2 m depth is about 200 kPa, whereas at the bottom of the pile this value is around 800–4000 kPa (see Fig. 20). Because there will be smaller soil strains at the lower depths than at the top, it is not possible to reach p_{ult} value in lower depths unless the topsoil undergoes a very large displacement such as 10–20% axial strain. Such large strains are not allowed in properly designed piles, therefore large p_{ult} values at lower depths in Fig. 20 are usually not encountered in practice.

The p_{ult} value for the same soil and pile was formerly demonstrated in Fig. 13. At the depths $x = 0.5$ m and $x = 1$ m, the ultimate lateral resistance value p_{ult} can easily be reached at smaller displacement values such as 0.02 m. However, for the depths greater than 1 m, p_{ult} value can not be reached within 0.02 m of displacement (see Fig. 13). Therefore, for the formula offered in this study, p_{ult} will be replaced with $p_{@disp}$, which indicates the soil resistance at a given displacement. $p_{@disp}$ values corresponding to displacement values 0.005 m, 0.01 m and 0.03 m respectively are plotted in Fig. 20. As shown in the figure, the $p_{@\%disp}$ value (lateral soil resistance at a certain percentage of pile displacement) exhibits high variability depending on the displacement. This variability indicates that the lateral soil resistance is not a constant value but rather changes as the pile undergoes different levels of displacement.

7 Conclusion

This study proposes empirical formulas based on finite element analysis (FE) to estimate p-y curves for piles embedded in sand, with a maximum depth of 20 m. The formulas take into account parameters such as soil modulus, friction angle, and pile diameter. The following statements can be made:

- The formula incorporates a wide range of parameters, including soil modulus, internal friction angle, and pile diameter. The FE-based p-y curves allow for modeling of elasto-plastic behavior, with the soil modulus influencing the estimation of these curves.
- When a horizontally loaded pile is considered, the p-y curves initially flatten at shallow depths but exhibit a more linear trend at greater depths. The depth at which the p-y curve flattens varies, unlike the current practice where a constant displacement value is assumed for the flattening point.
- The most significant factors influencing the p value are the internal friction angle of the soil and the pile diameter. Conversely, the soil unit weight has a relatively smaller effect.
- While the p value in kN/m increases with increasing pile diameter, the average lateral earth pressure (p/D) in kN/m^2 decreases as the diameter (D) increases.
- In 3D structural analysis software, piles beneath buildings are commonly represented as beam elements supported by springs. The provided formula can be utilized to calculate the spring coefficients for these pile models.
- In addition to horizontal springs, the piles are also supported by vertical springs. However, the force–displacement relations for the vertical springs have not been derived in this work. As a potential area for future research, it would be beneficial to investigate and develop the force–displacement relationships for these vertical springs.
- Modeling piles using beam and spring elements provides a certain level of accuracy; however, it is important to note that in reality, the soil is continuous, meaning the springs surrounding the piles are interconnected.

Supplementary Information The online version contains supplementary material available at https://doi.org/10.1007/s13369-023-08121-z.

Data availability Some or all data, models, or code generated or used during the study are proprietary or confidential in nature and may only be provided with restrictions (Output files of Midas GTS NX runs).

References

1. Clough, G. W., J. M. Duncan: Earth pressures. In: Foundation engineering handbook, edited by H. Y. Fang, 223–235. 2nd ed. New York: Chapman and Hall (1991)
2. Hamderi, M.: Finite element-based coefficient of lateral earth pressure for cohesionless soil. Int. J. Geomech. **21**(5), 04021045 (2021)
3. Brinch Hansen, J.: The ultimate resistance of rigid piles against transversal forces. Bulletin No. 12, Danish Geotechnical Institute, Copenhagen, Denmark, 5–9 (1961)
4. Broms, B.B.: Lateral resistance of piles in cohesive soils. J. Soil Mech. Found. Div. **90**(2), 27–64 (1964)
5. Fleming, W.G.K.; Weltman, A.J.; Randolph, M.F.; Elson, W.K.: Piling engineering. Surrey University Press, London (1992)
6. Reese, L. C., Cox, W. R., Koop, F. D.: Analysis of laterally loaded piles in sand. Proc., 6th Offshore Technology Conf., Vol. 2, Houston, 473–483 (1984)
7. Zang, L.: Lateral bearing behaviors of slightly inclined single pile with different pile head restraint under combined loads. Arab. J. Sci. Eng. (2020). https://doi.org/10.1007/s13369-020-05026-z
8. Chari, T.R.; Meyerhof, G.G.: Ultimate capacity of single piles under inclined loads in sand. Can. Geotech. J. **20**, 849–854 (1983)
9. Meyerhof, G.G.; Sastry, V.V.R.N.: Bearing capacity of rigid piles under eccentric and inclined loads. Can. Geotech. J. **22**, 267–276 (1985)
10. Meyerhof, G.G.; Mathur, S.K.; Valsangkar, A.J.: Lateral resistance and deflection of rigid wall and piles in layered soils. Can. Geotech. J. **18**, 159–170 (1981)
11. Khari, M.; Armaghani, D.J.; Dehghanbanadaki, A.: Prediction of lateral deflection of small-scale piles using hybrid PSO–ANN model. Arab. J. Sci. Eng. (2019). https://doi.org/10.1007/s13369-019-04134-9
12. Kim, B.T.; Kim, N.K.; Lee, W.J.; Kim, Y.S.: Experimental load-transfer curves of laterally loaded piles in Nak-Dong river sand. J. Geotech. Geoenviron. Eng. **130**(4), 416–425 (2004). https://doi.org/10.1061/(ASCE)1090-0241(2004)130:4(416)
13. Georgiadis, M.; Anagnostopoulos, C.; Saflekou, S.: Centrifugal testing of laterally loaded piles in sand. Can. Geotech. J. **29**(2), 208–216 (1992). https://doi.org/10.1139/t92-024
14. Klinkvort, R.T.; Hededal, O.: Effect of load eccentricity and stress level on monopile support of offshore wind turbines. Can. Geotech. J. **51**(9), 966–974 (2014). https://doi.org/10.1139/cgj-2013-0475
15. Bouzid, D.: A: analytical quantification of ultimate resistance for sand flowing horizontally around monopile: New p-y curve formulation. Int. J. Geomechanics (2021). https://doi.org/10.1061/(ASCE)GM.1943-5622.0001927
16. Ghorbanzadeh, M.; Sensoy, S.; Uygar, E.: Seismic performance assessment of semi active tuned mass damper in an MRF steel building including nonlinear Soil–Pile–structure interaction. Arab J Sci Eng (2023). https://doi.org/10.1007/s13369-022-07138-0
17. Reese, L. C., Sullivan, W. R: A Documentation of Computer Program COM624, Parts I and II, Analysis of Stresses and Deflections for Laterally Loaded Piles Including Generation of p-y Curves. Geotechnical Engineering Software GS80–1, Geotechnical Engineering Center, Bureau of Engineering Research, University of Texas at Austin (1980)
18. Bowles, J. E.: Foundation Analysis and Design, McGraw-Hill Inc., 5th 733 edition (1987)